PlGF Regulates Angiopoietin-1 and Tie-2 Expression in Human Retinal Endothelial Cell-Pericyte Cocultures and iPSC-Derived Vascular Organoids through VEGFR1

Hu Huang (huangh1@missouri.edu)
University of Missouri https://orcid.org/0000-0003-2843-0320
Madhu Saddala
MU: University of Missouri
Rajiv Ravindra Mohan
University of Missouri

Research Article

Keywords: Angiopoietin, blood-retinal barrier, diabetic macular edema, diabetic retinopathy, endothelial cell, induced pluripotent stem cells, pericyte, placental growth factor, retina, tie2, vascular endothelial growth factor receptor 1, vascular organoids

Posted Date: July 7th, 2021

DOI: https://doi.org/10.21203/rs.3.rs-651093/v1

Abstract

Placental growth factor (P*/*GF) and Angiopoietin (Ang)-1 are two angiogenic factors that play vital roles in vascular cell growth and stabilization. The present study's objective is to examine P*/*GF's regulation of Ang-1 and its Tie-2 receptor expression in human vascular cells and vasculature. We exploited the cocultures of human primary retinal endothelial cells (HREC) and pericytes (HRP) and the blood vessel or vascular organoids derived from human-induced pluripotent stem cells (iPSC) as experimental models. In the HREC-HRP cocultures, P*/*GF blockage upregulated the expressions of Ang-1 and Tie-2 in an antibody dose-dependent manner. Upregulation of Ang-1 and Tie-2 by P*/*GF blockade did not occur in HREC and HRP monocultures but only in HREC-HRP cocultures, indicating the interactions of the two cell types. VEGFR1 inhibition diminished Ang-1 and Tie-2 upregulation caused by P*/*GF blockade and reduced pericyte variability in high glucose conditions. In the iPSC-derived vascular organoids (VO), P*/*GF, Ang-1, and Ang-2 were expressed mainly by perivascular cells. Bioinformatics analysis of RNA sequencing data revealed that diabetes-mimicking conditions upregulated P*/*GF and Ang-2 expressions in the VO cultures. P*/*GF blockade upregulated Ang-1 and Tie-2 expression and promoted pericyte coverage and association with ECs in the VO. Together, the data suggest that P*/*GF regulates Ang-1 and Tie-2 expression in part through VEGFR1, which is involved in vascular cell function and stabilization. The findings may help design new therapeutic interventions for diabetic vasculopathy, such as diabetic macular edema and proliferative diabetic retinopathy, by targeting P*/*GF and Ang signaling pathways.

1. Introduction

Diabetic retinopathy (DR) is manifested clinically as a microvascular disorder caused by diabetes.[1] It is also complicated as retinal neurodegeneration, glial activation, and inflammatory response.[2,3] These early complications result in compromised visual function, oxidative stress, and chronic inflammation. Photoreceptors-derived oxidants are significant contributors to DR onset and progression.[4] Glial cell reactivation causes retinal inflammation by producing cytokines/chemokines, such as Tumor necrosis factor-alpha (TNF-α), Interleukin-6 (IL-6), and chemokine MCP-1 (CCL2).[5,6] At mild and moderate non-proliferative DR (NPDR), the retinal vasculatures are characterized with various degrees of vascular abnormalities, such as pericyte drop-off, dissolution of endothelial cells (ECs), and pericytes, acellular capillaries, microaneurysms, retinal hemorrhages, and intraretinal microvascular abnormalities.[7,8] As the disease progresses to severe NPDR, retinal microvascular capillaries become occluded, nonperfusion, retinal ischemia, and vascular leakage resulting from blood-retinal barrier (BRB) breakdown.[9] At the advanced stage of PDR, ischemic retinas produce pro-angiogenic factors, such as hypoxia-inducible factor (HIF)-associated vascular endothelial growth factor (VEGF), which drive microvascular endothelial cell proliferation, migration, angiogenic growth, and eventually generate pathological neo-vasculatures and grow across the inner limiting membrane into the humor vitreous. Diabetes-caused retinal vascular atrophies and dysfunction result in vision impairment and blindness, particularly from the forms of diabetic macular edema (DME) and proliferative DR (PDR).[1]

Increasing evidence supports that P*l*GF can be a therapeutic target to treat patients with PDR and DME.[10–12] P*l*GF is expressed in various retinal cells, such as vascular endothelial cells, pericytes, and retinal pigment epithelium (RPE), in DR and DME. P*l*GF has multiple functions by eliciting distinct intracellular signaling and downstream mechanisms. For example, P*l*GF can be pro-angiogenic through heterodimerization with VEGF-A and indirect activation of VEGFR2 signaling, or displacement of VEGF-A from the VEGFR1, thereby allowing VEGF-A to bind VEGFR2.[13] P*l*GF also mediates the inflammatory effect through VEGFR1 signaling in monocytes, microglia/macrophage, and endothelium, which are involved in DR development.[14,15] One study by Cao et al.[16] revealed that diabetes upregulates P*l*GF and phosphorylate VEGFR1, thereby activating the PKC-ERK1/2-NOS-1 signaling transduction pathway in human retinal endothelial cells (HREC) using siRNA against P*l*GF and PKC inhibitor (Go 6976). Another study by Lazzara et al.[17] showed that Aflibercept and selective P*l*GF inhibition by anti-P*l*GF antibody exerted a protective effect on human retinal pigment epithelial cells (RPE) and HREC from diabetes through the inhibition of the ERK1/2-NFκB-TNFα signaling pathway. Our study showed that P*l*GF blockade could promote the cultured EC's barrier function by suppressing glucose-6-phosphate dehydrogenase (G6PD)/pentose phosphate pathway (PPP)-related antioxidant defense.[18] These new *in-vitro* data corroborate our previous *in-vivo* findings of the protective role of P*l*GF deletion using diabetic P*l*GF KO mice (Akita.P*l*GF$^{-/-}$).[7]

Angiopoietin (Ang or Angpt) are secreted signaling glycosylated peptides and include four family members (Ang-1 ~ 4).[19] Ang-1 and Ang-2 have been mostly characterized and can competitively bind with the tyrosine kinase Tie-2 receptor.[20] Ang-1/2/Tie-2 signaling axis augments several downstream signaling pathways, such as PI3K/protein kinase B (Akt) and extracellular signal-regulated kinase (ERK) pathways.[21] This signaling axis plays a vital role in angiogenesis by regulating the number and diameter of developing vessels during embryonic development; it is also a key regulator of endothelial quiescence and survival in adult vasculatures.[22,23] In contrast, Ang-2 acts as a partial agonist/antagonist of Tie-2 signaling in the endothelial cells and pericytes.[24,25] Both vitreous and plasma Ang-2 level is upregulated in diabetic patients with NPDR, DME, or PDR.[26,27] Genetic and pharmacological studies revealed that Ang-2 could cause pericyte loss and BRB leakage, and act as a target for therapeutic intervention to treat PDR and DME.[28–30]

The present study was conducted to investigate P*l*GF's regulation of Ang-1/-2 and Tie-2 expression in the two culture systems. One is the cocultures of human retinal pericytes (HRP) and HREC; the other is the blood vessel or vascular organoids (VO) derived from human induced pluripotent stem cells (iPSC). The rationale of this study is to give insights into the relation of PlGF/VEGFR1 and Ang-1/Tie-2 using the cultured human retinal cells and vascular organoids, which have not been reported in the literature. More importantly, the recently developed three-dimensional (3D) human VO provides an attractive model system for diabetic vasculopathy. They are similar to human vasculatures, as demonstrated by vital vascular elements, vascular networks, and perfusion function.[31] Pericyte coverage and association with EC in the VO were examined with the relative expression and colocalization of PDGFRb relative to CD31.

The findings can potentially aid in the design of combination therapy for DR disease by targeting both P*/*GF and Ang signaling pathways.

2. Materials And Methods

2.1. Cell cultures and antibody treatments

The primary human retinal endothelial cells (HREC; Cat#: ACBR1 181) and human retinal pericytes (HRP; Cat#: ACBR1 183) were purchased from Cell Systems (Kirkland, WA) and cultured based on the experimental procedures as described previously.[18,32] In brief, HREC were seeded on fibronectin-coated (1µg/cm^2, Cat#: 1030-FN, R&D Systems). Plastic vessels and cultured with EBM2-MV medium (Cat#: cc-4176, Lonza) supplemented with EC growth factors (Cat#: cc-4147, Lonza). HRP cells were cultured with a complete pericyte culture medium (Cat#: 4N0-500, Cell Systems) with supplementation of normal glucose, culture boost (Cat#: 4CB-500, Cell Systems), and attachment factor (Cat#: 4Z0-201, Cell Systems). HREC and HRP cells were cocultured at the ratio of 2:1 with the combination of two culture media. After HREC monolayer formation and HREC-HRP coculture stabilization, the culture media were replaced with fresh ones with the following desired treatment agents: D-glucose (25 mM), mannitol (25 mM), hydrocortisone (50 mM), anti-P*/*GF antibody (PL5D11D4), and anti-VEGFR1 antibody (MF1, ImClone Systems). The treatment duration was 2 days. It is worth noting that the mouse anti-P*/*GF antibody was validated to bind with human P*/*GF protein in our previous study.[18] Both anti-P*/*GF and anti-VEGFR1antibodies showed robust efficacy in *in-vivo* and *in-vitro* experiments.[33,34]

2.2. Human iPSC-derived vascular organoids cultures

Human iPSC cells, reprogrammed from a non-disease human subject, were obtained from Infinity BiologiX LLC, NJ (Subject: NDS00249; iPSC: ND50018; Passage 11). The iPSC cells were cultured and maintained with the mTeSR1 medium (Cat#: 85850, STEMCELL Technologies), which was formulated from basal medium (Cat#: 85851 STEMCELL) and supplement (Cat#: 85852, STEMCELL). Blood vessel or vascular organoids were generated according to the protocols described by Wimmer et al.[31,35] Briefly, human iPSC cells were first aggregated on a 6-well low attachment plate with the mTeSR1 medium containing 50 µM Y27632 (ROCK inhibitor, Cat#: 688001, Calbiochem, Millipore/Sigma) for 1 day. Then, the iPSC cell aggregates were committed to mesoderm linage in the presence of 12 µM CHIR99021 (GSK3β inhibitor, Cat#: 4423, Tocris) and 30 ng/mL BMP-4 (Cat#: 78211, Stemcell Tech) for 3 days. The aggregated progenitor cells were further differentiated into vascular cells with 100 ng/ml VEGF-A and 100 ng/ml FGF-2 for 2 days. The final step was that vascular cells continue to sprout, grow and form a network in the collagen I-Matrigel matrix under the induction of VEGF-A and FGF-2 from 5 to 14 days. The success of vascular organoids was confirmed by 3-dimensional (3D) structures, vascular network, and pericyte coverage (Suppl. Figure 1 and Suppl. Figure 2).

2.3. Trans-endothelial electrical resistance measurement by an electrical cell-impedance sensing system

HRECs and HRP were seeded and cocultured at 2:1 ratio on the 8-well cultureware (PC, 8W10E). Trans-endothelial electrical resistance (TEER) changes were measured in real-time with the electrical cell-impedance sensing system (ECIS)-Z system (Applied Biophysics, NY). The ECIS software embedded mathematical model of impedance change was used to calculate the TEER (Ω/cm^2), measuring the cell-cell barrier and cell-matrix resistance functions.[36] The single frequency model (4000 Hz) was used to measure resistance and impedance with a 300s interval. After the resistance stabilized and reached a platform, indicating the formation of confluent monolayer and functional barrier, The various treatments: IgG control, P*l*GF antibody (50 µg/ml), and P*l*GF antibody (50 µg/ml) + VEGFR1 antibody (50 µg/ml) was added to the medium and then continued to culture for two days. The normalized resistance values were expressed as a percentage relative to vehicle control.

2.4. Western blot and densitometric quantification

Western blot (WB) was performed according to the previously described methods with some modifications.[18,34,37] HREC and RRP were mono- and cocultured to confluency in 6-well plates and used for WB analysis. In brief, the cells were washed with cold PBS three times, detached with a cell scraper, and collected by centrifugation. The harvested cell pellets were sonicated in cold RIPA buffer containing FAST protease inhibitors (Cat#: S8830, Sigma, St. Louis, MO). The protein concentration was determined with the DC™ Protein Assay kit (Bio-Rad) and Qubit 4 fluorometer.

Before the electrophoretic transfer to 0.45 µm pore-size nitrocellulose membranes, 30–50 µg total protein per lane were separated by 4–20% sodium dodecyl sulfate-polyacrylamide gel electrophoresis (SDS-PAGE). The membranes were blocked with 5% non-fat milk (Bio-Rad) or 2% BSA at room temperature for 1 hr and then incubated overnight at 4°C with the following primary antibodies: anti-Ang-1 (1:500, Cat#: A7877, Abclonal, Boston, MA; Species Reactivity: Human, Mouse, Rat); anti-Ang-2 (1:500, Cat#: A0698, Abclonal; Species Reactivity: Human, Mouse, Rat); anti-Tie-2 (1:500, Cat#: ab24859, Abcam; Species Reactivity: Human); anti-VE-cadherin (1:1,000, Cat#: 5012896, Thermo-Fisher; Species Reactivity: Human), anti-N-cadherin (1:1,000, Cat#: 33-3900, Thermo-Fisher; Species Reactivity: Human, Mouse, Rat, Chicken, Porcine), and anti-GAPDH (1:1,000, Cat#: G9545, Sigma; Species Reactivity: Human, Mouse, Rat). After being washed with PBST buffer, the membranes were incubated with horseradish peroxidase (HRP)-conjugated secondary antibody (1:2000; Cell Signaling Technology) for 1 hr at room temperature. Signals were developed with enhanced chemiluminescence with a SuperSignal West Pico kit (Thermo-Fisher) and detected with an ImageQuant LAS 500 (GE Healthcare). Densitometry analysis was performed through the use of ImageJ software (NIH, Bethesda). All the quantification results were averaged from 3 protein blots and expressed as the mean ratio of the target protein GAPDH ± standard deviation (SD) unless otherwise specified.

2.5. RNA Isolation and Quantitative Real-Time PCR (qRT-PCR)

qRT-PCR was conducted accruing to the previously described protocol with some modifications[38].

Vascular organoids were washed with PBS, and total RNA extracted using RNeasy Plus Mini Kit; (Qiagen) according to the kit protocol with addition RLT plus buffer supplemented with 20ul of 2M Dithiothreitol (DTT). RNA was analyzed for quality and quantified using a NanoDrop One (Thermo Fisher Scientific) and reverse transcribed to cDNA using Maxima™ H Minus cDNA Synthesis Master Mix, with dsDNase (M1682; Thermo Fisher Scientific), according to the manufacturer's protocol in SimpliAmp Thermal Cycler; (Life Technology, MA, USA). Gene expression analysis was performed using Power SYBR Green Master Mix (Thermo Fisher Scientific) with the following mouse-specific primers: Ang-1 (#BC152419.1: forward: AGAAGGTGTTTTACTAAAGGGAGG, reverse: CAGTCCAACCTCCCCCATTG,), Tie-2 (#BC035514.1: forward: GTTCTGTCTCCCTGACCCCT, reverse: TGGAAGCGATCACACATCTCC), and Cyclophilin (forward: CAGACGCCACTGTCGCTTT, reverse: TGTCTTTGGAACTTTGTCTG) in a Quant Studio 3 RT-PCR system (Applied Biosystems, CA, USA). The relative expression values of target genes were normalized to Cyclophilin as the housekeeping gene, and the fold change was calculated using the relative quantification ($2^{-\Delta\Delta CT}$) method. Four biological replicates per treatment group were run in three technical replicates.

2.6. Immunofluorescence staining analysis

HRP cells and vascular organoids (VO) were cultured as described above. At the experiments' endpoints, the cells and VO samples were cryo-sectioned or flat-mounted, fixed in 4% paraformaldehyde (VVR Life Science), permeabilized by incubation in 0.05% Triton X-100, and blocked with 10% normal goat serum (NGS). The fixed samples were then incubated with the desired primary antibodies. For the HRP staining, anti-cleaved caspase-3 antibody (1:100, Asp175, Cat#: 9661, Cell Signaling) and anti-RPE65 antibody (1:50, Cat#: MA1-16578, Thermo-Fisher; Species Reactivity: Bovine, Dog, Chicken, Human, Mouse, Pig, Rat, Xenopus) were used. For the VO staining, the following antibodies were used: anti-CD31(1:100, Cat#: 375902, BioLegend; Species Reactivity: Human), anti-PDGF receptor beta (PDGFRb, 28E1, 1:100, Cat#:3169S, Cell Signaling; Species Reactivity: Human, Mouse, Rat), anti-Collagen IV (Col IV, 1:100, Cat#: MA1-22148, Invitrogen; Species Reactivity: Human, Rat), anti-Ang-1 (1: 100, same as WB), and anti-Tie-2 (1: 100, same as WB). After washing with PBST buffer, the staining signals were visualized by goat anti-rabbit IgG (H + L) Cyanine5, goat anti-mouse IgG (H + L) Alexa Fluor 488, and goat anti-rat IgG (H + L) pacific blue. The cell nuclei were stained with DAPI (1:5,000). The slides were mounted with a ProLong Diamond antifade reagent (Thermo-Fisher) and imaged with an LSM 700 inverted laser confocal microscope (Carl Zeiss, Oberkochen, Germany).

2.7. TUNEL Assay for Detection of Apoptotic Nuclei

The terminal dUTP nick-end labeling (TUNEL) assay was performed according to previously described procedures with some modifications using the commercial kit (ApopTAG Red In Situ Apoptosis Detection Kit; Millipore, Temecula, CA).[6] In brief, The cells were fixed in 1% paraformaldehyde for 10 minutes at room temperature and then washed twice for 5 minutes in PBS (pH7.4). After the tailing of digoxigenin-dNTP catalyzed by the TdT enzyme, the sections were incubated with the anti-digoxigenin-rhodamine antibody for 30 minutes at room temperature. The processed specimen was mounted with the antifade

mounting medium for fluorescence-containing DAPI (Vectashield; Vector, Burlingame, CA) and viewed fluorescence microscope.

2.8. Cytotoxicity assay of the HRP cell cultures.

HRP cells were cultured in 96 well plates with normal glucose (5 mM D-glucose + 20 mM mannitol) and high glucose (25mM D-glucose) with or without anti-VEGFR1 antibody (50 μg/ml) for 5 days. MTT assay was performed to quantitively evaluate the cell viability caused by high glucose and anti-VEGFR1 ab. The resultant absorbances were read at 570 nm using 800 TS Absorbance Reader (BioTek Instruments, Winooski, VT, USA). The absorbance of 650 nm was used as a reference wavelength.

2.9. Colocalization analysis of the double-stained vascular organoids

The vascular organoids treated IgG control, and P*/*GF ab was immuno-stained with the primary antibodies against EC marker CD31 and pericyte marker PDGFRb and the secondary goat anti-rabbit IgG (H + L) Cyanine5, goat anti-mouse IgG (H + L) Alexa Fluor 488. Immunofluorescence images were taken with EVOS M7000 fluorescent microscopy. The colocalization correlation between green and red signals was analyzed by the JACoP (Just Another Co-localization Plugin) plugin of ImageJ software. Briefly, after being imported into ImageJ software, the two channels were converted to 8-bit for analysis. Then, the JACoP plugin was used for colocalization analysis between two channels (green and red) followed by an online document (https://imagej.nih.gov/ij/plugins/track/jacop2.html). Pearson's correlation coefficient and Manders' Coefficients (M1 & M2 overlay coefficients) with Costes' automatic threshold in the result panels were used for further statistical analysis.

2.10. Bioinformatics analysis of RNA sequencing data

RNA-Seq datasets are taken from the Sequence Read Archive (SRA) (https://www.ncbi.nlm.nih.gov/ sra/? term = SRP092491) from the National Centre for Biotechnology Information (NCBI). Wimmer et al. 2019 produced the original datasets and deposited them in SRA (Bioproject: PRJNA352279)[31]. The dataset information describe briefly as follows, vascular organoids were differentiated from human iPS cells and treated for 3 weeks with a diabetic media containing 75mM Glucose, 1ng/mL TNF-α, 1ng/mL IL6 (DI) or left untreated in 17mM Glucose (NG). Endothelial cells were FACS sorted for CD31 directly into Trizol and stored at -80°C before RNA preparation. The two NG (Normal Glucose) and 2 DI (Diabetes Induced) are pools of sorted endothelial cells from multiple vascular organoids (> 100) from 2 independent differentiations/treatments.

Raw reads were mapped to the genome (hg19) using HISAT2 0.1.6[39]. Only reads with unique mapping were considered for further analysis. Gene expression levels were calculated using the HISAT2 software package (http://daehwankimlab.github.io/hisat2/). Normalization and differential expression analysis were done using the DESeq2 R package (Bioconductor, https://bioconductor.org/packages/release/ bioc/html/ DESeq2.html). Differentially expressed genes were selected using a twofold change cut-off

between at least two populations and P < 0.05 adjusted for multiple gene testing. The Gene expression matrix was clustered using a k-means algorithm with correlation as the distance metric.

3. Statistical Analysis

The values were expressed as the mean ± standard deviation (SD) for the respective groups. Statistical analyses were performed with GraphPad Prism 8 software. Analysis of variance (ANOVA) or a linear mixed model was used for the statistical comparisons of multiple groups.[40] The *p*-values for the comparison of the treatments were adjusted for multiple comparisons with Dunnett's test. The non-parametric Mann–Whitney U test was performed to determine the significance level between the two groups. Statistical significance was set at $p < 0.05$.

4. Results

4.1. P*/*GF blockade regulates Ang-1 and Tie-2 in HREC-HRP cocultures in an antibody concentration-dependent manner

To investigate whether P*/*GF is involved in pericyte-endothelial interactions, we first examined the effect of PlGF blockade on the expression levels of Ang-1, Tie-2, VE-Cadherin, and N-Cadherin proteins in the HREC-HRP cocultures. The confluent cocultures were treated with the neutralizing P*/*GF antibody (PL5D11D4) at three concentrations (25, 50, and 100 µg/ml) for two days. WB analysis was performed to examine the protein expression changes. WB barely detected Tie-2 protein expression at the vehicle control samples (Fig. 1A). The P*/*GF antibody at the dose of 25 µg/ml slightly increased the Tie-2 protein level compared with vehicle control. 50 and 100 µg/ml antibody doses upregulated the Tie-2 protein expression compared with vehicle control and 25 µg/ml antibody. WB detected N-Cadherin, VE-Cadherin, and Ang-1 protein expressions in all four groups (Fig. 1A and B). 25 µg/ml P*/*GF antibody decreased the protein abundance of N-Cadherin (N-Cad) and Ang-1 but not VE-Cadherin (VE-Cad) compared with vehicle control. 50 and 100 µg/ml P*/*GF antibody concentrations upregulated protein levels of Ang-1 but not N-Cad or VE-Cad compared with control and 25 µg/ml antibody. The protein blots were quantified to determine whether there are significant differences between treatment groups. The quantitative results (Fig. 1C & D) revealed no significant differences for Tie-2 between vehicle control and 25 µg/ml antibody, between 50 and 100 µg/ml P*/*GF antibody. However, the two higher antibody doses (50 and 100 µg/ml) significantly upregulated Tie-2 protein expression compared with the lower antibody dose (25 µg/ml) and control conditions. 25 µg/ml P*/*GF antibody downregulated N-cadherin compared with vehicle control. There were no significant differences for VE-cadherin between any groups. 25 µg/ml antibody downregulated, but the two higher doses upregulated Ang-1 compared with vehicle control. These results indicate that P*/*GF regulates the protein expressions of Ang-1 and Tie-2 but not N-Cad or VE-Cad depending on antibody concentration.

4.2. Ang-1 upregulation by PlGF blockade in HREC-HRP cocultures, but not monocultures

It is well established that Ang-1 is secreted by the peri-endothelial cells such as pericytes regulate Tie-2 signaling activity in endothelial cells in a paracrine manner.[41] Therefore, we examined whether upregulation of Ang-1 protein expression by P/GF blockade requires HREC-HRP interactions. The confluent HREC, HRP mono- and cocultures were treated with 50 μg/ml P/GF antibody for two days (the effective dose from above). The western blots detected Ang-1 protein expression in all three types of cultures: HRP monoculture, HREC monoculture, and HRP-HREC cocultures (Fig. 2A-C). P/GF antibody upregulated Ang-1 protein expression in the HRP-HREC cocultures but not the two monocultures compared to vehicle control. Further densitometry quantification of protein blots confirmed a significant difference between the P/GF antibody and IgG control in the cocultures but not the monocultures (Fig. 2D-F). We also examined the expression of Ang-2 protein (a partial agonist/antagonist of Tie-2) and the effect of P/GF inhibition in the three culture systems. Ang-2 expression was detected in the HRP-HREC cocultures and HRP monocultures. However, WB failed to detect Ang-2 expression in HREC monocultures. Because that ECs could express and store Ang-2[25], it should be cautious about interpreting this result, possibly caused by the expression level of Ang-2 that is not enough for the immunoblotting to detect in the cultured HRECs. WB and densitometry analyses revealed P/GF inhibition does not alter Ang-2 protein expression in all three culture systems compared with vehicle control. These results indicate that Ang-1 upregulation by PlGF blockade is dependent on EC-pericytes interactions, and the relative ratio of Ang-1 to Ang-2 was increased due to the Ang-1 upregulation and Ang-2 non-alteration which may contribute to the beneficiary effect of P/GF blockade on EC integrity and function, as we reported previously[18].

4.3. VEGFR1 is involved in P/GF's effect on Ang-1 and Tie-2 expression and EC barrier function

P/GF confers function (i) directly through VEGFR1, (ii) through heterodimerizing with VEGF-A and activation of VEGFR1 and R2, or (iii) through replacing VEGF-A from VEGFR1 to VEGFR2, then indirectly activating VEGF-A/VEGFR2 signaling. We asked what mechanism through which P/GF regulates Tie-2 and Ang-1 gene expression and EC barrier function. First of all, we found that VEGFR1 inhibition reduced the increased Tie-2 and Ang-1 protein levels caused by P/GF blockade compared to the vehicle control, suggesting that VEGFR1 is involved in the expression regulation (Fig. 3A, B). VEGFR1 inhibition also reduced EC barrier function, as indicated by reduced resistance (Fig. 3C). Since VEGFR1 inhibition antagonizes the effects of P/GF blockade, it is unlikely that P/GF exerts this function directly via VEGFR1 or heterodimerizing with VEGF-A and activating both VEGFR1 and R2 receptors. Therefore, it is reasonable to infer that P/GF blockade upregulates Ang-1 and Tie-2 expression and promotes EC barrier function indirectly through activating VEGF-A/VEGFR1 signaling: P/GF blockade makes more VEGFR1 available to VEGF-A; thus VEGFR1 blockade attenuates P/GF's promoting effect on gene expression and barrier function. Whether VEGFR2 is also involved is unclear and needs further investigation.

4.4. VEGFR1 inhibition reduces pericyte viability in high glucose condition

We next investigated whether VEGFR1 mediates pericytes viability in high glucose (HG, diabetes-like) conditions in cell cultures. HG treatment reduced viability, as shown by LDH and MTT results (Fig. 4A, B). Apoptotic cells were significantly increased in HG + VEGFR1 inhibition conditions than normal glucose control and HG condition (Fig. 4C), indicating VEGFR1's involvement in pericyte survival. Additionally, by using an anti-phospho-(p)VEGFR1 antibody, we found that the phosphorylated or activated VEGFR1 form was co-localized with the apoptotic cells (either Caspase 3^+ or $TUNEL^+$) induced by HG (Fig. 4D-F).

4.5. Upregulation of P*/*GF and Ang-2 by the diabetes-mimicking condition in vascular organoids

Blood vessel or vascular organoids have recently been created from human ESC and iPSC as an appealing model for diabetic vasculopathy.[31,35] By using the protocols provided by the authors, we have successfully generated 3-dimensional (3D)-VO from human iPSC, which are structurally and functionally similar to human vasculatures and contain the key vascular components, including CD 31 (+) EC-formed vessel lumen structures, the associated PDGFRb (+) pericytes, and the Col IV (+) basements deposits (Suppl Fig. 1 and reference [42]). Using the RNA sequencing data of the VO treated with diabetes-like conditions versus normal medium available from the public database,[31] we first performed bioinformatics data analysis. The results revealed that both P*/*GF and Ang-2 were significantly upregulated in the diabetes-mimicking treatment group compared to the control group (Fig. 5A-C). Then, we examined their expression in the VO using the double immunofluorescence staining. The results revealed that P*/*GF and Ang-2 were expressed in perivascular cells associated with $CD31^+$ ECs (Fig. 5D-I). The double stain of PlGF and Ang-2 showed the two factors had similar but not identical expression patterns (Fig. 5J-L), indicative of heterogenous peri-vascular cell types, such as pericytes, smooth muscle cells, and others. Higher magnification images (Suppl. Figure 3) further showed the two factors' peri-vascular (pericyte) and heterogeneous cell expressions.

4.6. P*/*GF blockade upregulates Ang-1 and Tie-2 in human iPSC-derived vascular organoids

We further examined whether the P*/*GF blockade could upregulate Ang-1 and Tie-2 in human iPSC-derived vascular organoids, As P*/*GF antibody at 50 µg/ml for 2 days was effective in the human EC-pericyte cocultures, we, therefore, doubled the antibody amount and treatment duration (100 µg/ml, 4 days) for the vascular organoids. The treated vascular organoids were cryopreserved and sectioned for the double immunofluorescence staining analysis of Tie-2 and Ang-1. The results showed the increased staining signal intensity in the P*/*GF ab treatment group compared with the IgG control (Fig. 6A, B, and Suppl. Figure 4). Ang-1 and Tie 2 staining signals were higher than secondary antibody controls (Suppl.

Figure 5). The quantification of staining intensity revealed the increased Ang-1 and Tie-2 expression levels by P/GF ab treatment compared to the vehicle control (Fig. 6C). qPCR further confirmed the mRNA transcripts of Ang-2 and Tie-2 were also upregulated in the antibody treatment relative to the control (Fig. 6D).

4.7. P/GF blockade promotes pericyte coverage and EC-pericyte association in vascular organoids

Finally, we investigated whether P/GF blockade promotes pericyte coverage and pericyte-EC association in vascular organoids, which was evaluated with the expression levels and correlation coefficiency of the PDGFRb's staining signal relative to the CD31's. The two-channels images have been calculated for relative expression and colocalization: the green channel for pericytes and the red channel for ECs (Fig. 7A-C). We used Image J with the JACop plugin to calculate Manders' overlap coefficient, which indicates the co-relations of the green (M1) and the red (M2). The M1 value for the green channel is 0.59 ± 0.5, and the M2 value for the red channel is 0.99 ± 0.0006 in the PBS control group. The M1 is 0.89 ± 0.13, and the M2 is 0.99 ± 0.0017 in PlGF-ab treated group (Fig. 7D). As indicated by cytofluorogram (Fig. 7E, F), P/GF ab treatment caused an increased Pearson's correlation coefficient of green signal versus red signals, which indicates that the P/GF blockade leads to increased coverage and colocalization of pericytes and ECs on organoid vasculatures.

5. Discussion

The present study's primary findings include 1) P/GF blockade upregulates Tie-2 and Ang-2 expression in both HREC-HRP coculture and human iPSC-derived vascular organoids, 2) VEGFR1 is involved in P/GF's regulation of Tie-2 and Ang-2 expression, 3) VEGFR1 inhibition reduces pericyte cell viability in high glucose condition, 4) P/GF and Ang-2 are expressed in perivascular cells and upregulated by diabetes-mimicking conditions in the VO, and 5) P/GF blockade promotes pericyte coverage and association with ECs in the VO. To our knowledge, this study is the first to illustrate the direct regulation of the two signaling axis in human retinal cells and VO vasculatures. The data highlight P/GF's regulation of Ang-1 and Tie-2 in human cells and vascular organoids. The significance of the two signaling pathway regulation is relevant to stabilize the endothelium, facilitating vascular function by enhancing pericyte coverage and association with ECs.

The extent of P/GF inhibition by the varying antibody concentrations affects the regulation of Ang-1 and Tie-2 gene expression. On the one hand, P/GF inhibition at a higher antibody dose (e.g., 50 µg/ml) leads to upregulated expression of Ang-1 and Tie-2, which is functional on EC-pericyte interaction and vascular stabilization. On the other hand, P/GF inhibition at a lower antibody dose (e.g., 25 µg/ml) causes a reduction of N-Cadherin, which is highly expressed in mesenchymal cells, thus acting as one marker of the endothelial-to-mesenchymal transition (EndMT)[43,44] and epithelial-to-mesenchymal (EMT)[45,46]. Therefore, this result suggests that P/GF inhibition at a low level might be involved in reducing EndMT. The observation that upregulation of Ang-1 occurred only in HREC-HRP coculture but not monoculture

suggests that a positive feedback loop may exist between pericytes and ECs. For example, the secreted pericyte Ang-1 activates Tie-2 in the ECs; subsequently, the activated Tie-2 triggers the signaling cascades in the ECs that in turn upregulate Ang-1 expression in the pericytes. These findings agree with our previous *in-vivo* study showing that P*gf* gene knockout prevents diabetes-caused pericyte loss and upregulates Ang-1 expression in the retina using diabetic P*l*GF knockout (Akita.P*l*GF$^{-/-}$) mice.[7]

To further confirm the regulatory mechanism observed in 2D cocultures of human retinal EC and pericytes, we exploited 3D vascular organoid cultures derived from human iPSC. As shown in Suppl Fig. 1, 3D vascular organoids contain the critical vascular components similar to human vasculatures, including the lumen-forming ECs, the closely associated pericytes, and the deposited basements, similar to those described by Wimmer et al.[31,42] Vascular organoids are physiologically more similar to the *in-vivo* vascular organs than the traditional 2D cell cultures, representing a new attractive model system to study vascular biology and screen new drugs for vasculopathy. Moreover, iPSC can be derived from human patients, which render the patient-derived vascular organoids (PDVO) powerful tools to mimic vascular diseases, screen drugs, and design personalized or precision medicine to treat vascular diseases, such as cardiovascular diseases, diabetic complications, and ischemic stroke. In the present study, we used human iPSC-derived vascular organoids to evaluate the pericyte-endothelial interaction by P*l*GF and Ang signaling pathways. Furthermore, we performed transcriptome bioinformatic analysis for the RNA sequencing data from the blood vessel organoids treated with diabetic conditions (high glucose + TNF-alpha + IL-6) versus vehicle controls.[31] The results revealed that both P*l*GF and Ang-2 are significantly upregulated in the blood vessel organoids by diabetic condition.

It is well established that Ang-1 protein secreted by perivascular cells such as pericytes, smooth muscle cells, and mesenchymal stem cells (MSC) activates Tie-2 signaling in the ECs and pericytes.[24] The paracrine and autocrine regulations of Tie-2 signaling activation are crucial for vascular maturation and junction formation during the late stage of angiogenesis and vascular remodeling.[47] Due to the complementary role to the VEGF signaling pathway, which essentially promotes angiogenic EC sprunting and proliferation and early vascular network formation during angiogenetic processes, there are combination therapy trials that simultaneously modulate both pathways to generate healthy and more normalized therapeutic neo-vessels rather than pathological leaky new vessels.[48,49] Deregulation of the Ang-1/Tie-2 signaling axis is implicated in DR pathogenesis, such as pericyte dropout, increased vascular permeability, BRB breakdown, and pathological angiogenesis.[21] The present study provides new insights into the regulation of Ang-1 and Tie-2 expression by P*l*GF-VEGFR1 signaling. Interestingly, our recent study found that both retinal pericytes and ECs express P*l*GF and VEGF-A. They form P*l*GF/VEGF-A heterodimers that mediate retinal EC barrier dysfunction via NF-κB.[18,32] Whether these molecular events are involved in the regulation of Ang-1 and Tie-2 expression is to be investigated.

Modulation of P*l*GF and Ang (Ang-1 and Ang-2) protein levels has been emerging as an attractive strategy to design new treatments for DR and DME.[21] Two phase-2 clinical trials (NCT03071068, NCT03499223) are underway to evaluate the safety and efficacy of a humanized P*l*GF antibody (THR-317) in the

treatment of DR and DME. Two large-scale phases 3 clinical trials (NCT03622580, NCT03622593) evaluate the efficacy, safety, and durability of the bispecific molecule (Faricimab), which targets VEGF-A and Ang-2, for the treatment of wet age-related macular degeneration (AMD) and DME compared to Aflibercept, which targets VEGF-A and P*l*GF. The present study investigated P*l*GF's regulation of the Ang-1 and Ang-2 expression in the HREC-HRP cocultures and the vascular organoids derived from human iPSC. Herein, we provided evidence suggesting that P*l*GF blockade enhances EC-pericyte interactions through control of the Ang-1/Tie-2 signaling axis. VEGFR1 acts as one downstream molecule of P*l*GF signaling to mediate cell viability and Ang-1 expression in the pericyte. The secreted Ang-1 promotes vascular stability by activating Tie-2 signaling cascades in both ECs and pericytes.[50] Although N-Cadherin and VE-Cadherin are the two key adherent molecules that participate in the EC-pericyte association and EC-EC junction, their protein expression levels were not altered by the P*l*GF blockade. It is possible that gene expression (transcription and translation)-independent mechanism of N-Cadherin and VE-Cadherin, such as post-translational phosphorylation and intracellular internalization, is involved downstream effect on EC function caused by P*l*GF blockade.[51]

In type 2 diabetic mellitus (T2DM), plasma P*l*GF concentrations are elevated before pathologic angiogenesis occurrence, suggesting that P*l*GF may serve as a potential biomarker for diagnosis of microvascular complication in T2DM patients.[52] Vitreous levels of P*l*GF significantly ($p < 0.05$) correlated with pathological angiogenesis and VEGF levels in diabetic patients with active PDR, and its receptor VEGFR1 (or FLT1) were detected in the ECs of proliferative neovasculature.[53] Another study also reported that vitreous P*l*GF levels are significantly higher in diabetic patients with DR than without DR.[54] These studies with clinical samples indicated that P*l*GF/VEGFR1 signaling is involved in the retinal microvascular complications both NPDR and PDR. As mentioned above, PlGF could contribute to DR pathogenesis through VEGFR1-mediated chronic inflammation. Additionally, P*l*GF could induce connective tissue growth factor (CTGF) expression in retinal vascular cells.[55] Given the multiple roles of the P*l*GF/VEGFR1 signaling pathway in various pathological conditions, its intervention may improve the outcome in DR patients by preventing vascular leakage, pathological angiogenesis, chronic inflammation, and angio-fibrotic switch.

Study limitations

there are several limitations from the present study. First, how P*l*GF blockade causes upregulation of Ang-1 expression in the pericyte is unclear. VEGFR1 is involved in the regulation, but whether it mediates directly or indirectly via VEGFR2 needs further elucidation. Also, whether other VEGFR ligands such as VEGF-A and VEGF-B and what target molecules (e.g., transcription factors) mediate the crosstalk between the two signaling pathways are to be characterized. Second, what downstream molecular events of the Ang-1 and Tie-2 signaling axis are involved in pericyte-endothelial interaction and EC barrier function need further investigation. It is well known that VE-Cadherin and N-Cadherin are effector molecules of the two signaling pathways. The two adhesion molecules' expression levels were not robustly altered by the P*l*GF blockade, suggesting that post-translational mechanisms may be involved. Since the

phosphorylation and internalization of the two adhesion molecules participate in vascular function mediated by signaling pathways, such as Sema4D/PlexinB1 signaling[56] and Erythropoietin (EPO),[57] it is possible that similar mechanisms are the downstream effects of PlGF-VEGFR1 and Ang-1/Tie-2 signaling crosstalk. Third, both P*l*GF and Ang-1 can play roles in pericyte and EC function via an autocrine and paracrine mechanism.[25,50] How the two pathways coordinate and contribute to vascular stability and function remains unclear. Lastly, we used a single antibody dose (100 µg/ml, 4 days) to treat vascular organoids. Despite effectiveness, the varying dose curve, incubation time, pharmacokinetics need to further define the new 3D organoids culture system.

Conclusions

The present study demonstrates crosstalk of the two signaling pathways of P*l*GF-VEGFR1 and Ang-1/Tie-2, regulating the EC-pericyte interaction and EC barrier function. We conformed the paracrine regulatory mechanism using both human retinal EC-pericyte coculture and iPSC-derived vascular organoids. Further investigations are needed to elucidate the regulatory mechanisms and promote translational potentials by targeting P*l*GF and Ang-1 signaling pathways.

Declarations

Ethics approval and consent to participate

Not applicable

Consent for publication

Not applicable

Availability of data and materials

All data that support the findings of this study are available from the corresponding author upon reasonable request.

Competing interests

The authors declare that they have no competing interests.

Funding

This work was supported by NIH R01 grant (EY027824, H.H.) and the Missouri University start-up fund (H.H.)

Authors' contributions

The study was conceived and designed by H.H. M.S.S. has performed quality checks, reference genome assembly, gene expression analysis, gene ontology, functional pathway analysis. M.S.S and H.H. have

conducted DESeq2 and R program analysis and conducted figures design and statistical analysis. The manuscript was written by M.S.S, H.H., and critically revised by H.H. Both authors reviewed and accepted the final version of the manuscript.

Acknowledgments

The authors like to acknowledge the contributions of Ms. Lijuan Fan (a lab technician) for technique assistance with iPSC-derived vascular organoid cultures and Dr. Anton Lennikov (a former postdoctoral fellow in our lab) for imaging with confocal microscopy.

References

1 Antonetti, D. A., Klein, R. & Gardner, T. W. Diabetic retinopathy. *N Engl J Med* **366**, 1227-1239, doi:10.1056/NEJMra1005073 (2012).

2 Ghirlanda, G., Di Leo, M. A., Caputo, S., Cercone, S. & Greco, A. V. From functional to microvascular abnormalities in early diabetic retinopathy. *Diabetes Metab Rev* **13**, 15-35, doi:10.1002/(sici)1099-0895(199703)13:1<15::aid-dmr176>3.0.co;2-m (1997).

3 Barber, A. J. & Baccouche, B. Neurodegeneration in diabetic retinopathy: Potential for novel therapies. *Vision Res* **139**, 82-92, doi:10.1016/j.visres.2017.06.014 (2017).

4 Du, Y., Veenstra, A., Palczewski, K. & Kern, T. S. Photoreceptor cells are major contributors to diabetes-induced oxidative stress and local inflammation in the retina. *Proc Natl Acad Sci U S A* **110**, 16586-16591, doi:10.1073/pnas.1314575110 (2013).

5 Miller, W. P. *et al.* Deletion of the Akt/mTORC1 Repressor REDD1 Prevents Visual Dysfunction in a Rodent Model of Type 1 Diabetes. *Diabetes* **67**, 110-119, doi:10.2337/db17-0728 (2018).

6 Huang, H. *et al.* TNFalpha is required for late BRB breakdown in diabetic retinopathy, and its inhibition prevents leukostasis and protects vessels and neurons from apoptosis. *Invest Ophthalmol Vis Sci* **52**, 1336-1344, doi:10.1167/iovs.10-5768 (2011).

7 Huang, H. *et al.* Deletion of placental growth factor prevents diabetic retinopathy and is associated with Akt activation and HIF1alpha-VEGF pathway inhibition. *Diabetes* **64**, 200-212, doi:10.2337/db14-0016 (2015).

8 Hu, J. *et al.* Inhibition of soluble epoxide hydrolase prevents diabetic retinopathy. *Nature* **552**, 248-252, doi:10.1038/nature25013 (2017).

9 Duh, E. J., Sun, J. K. & Stitt, A. W. Diabetic retinopathy: current understanding, mechanisms, and treatment strategies. *JCI Insight* **2**, doi:10.1172/jci.insight.93751 (2017).

10 Nguyen, Q. D. *et al.* Placental growth factor and its potential role in diabetic retinopathy and other ocular neovascular diseases. *Acta Ophthalmol* **96**, e1-e9, doi:10.1111/aos.13325 (2018).

11 Van Bergen, T. *et al.* The role of placental growth factor (PlGF) and its receptor system in retinal vascular diseases. *Prog Retin Eye Res* **69**, 116-136, doi:10.1016/j.preteyeres.2018.10.006 (2019).

12 Diabetic Retinopathy Clinical Research, N. *et al.* Aflibercept, bevacizumab, or ranibizumab for diabetic macular edema. *N Engl J Med* **372**, 1193-1203, doi:10.1056/NEJMoa1414264 (2015).

13 Carmeliet, P. *et al.* Synergism between vascular endothelial growth factor and placental growth factor contributes to angiogenesis and plasma extravasation in pathological conditions. *Nat Med* **7**, 575-583, doi:10.1038/87904 (2001).

14 Incio, J. *et al.* PlGF/VEGFR-1 Signaling Promotes Macrophage Polarization and Accelerated Tumor Progression in Obesity. *Clin Cancer Res* **22**, 2993-3004, doi:10.1158/1078-0432.CCR-15-1839 (2016).

15 Albonici, L., Giganti, M. G., Modesti, A., Manzari, V. & Bei, R. Multifaceted Role of the Placental Growth Factor (PlGF) in the Antitumor Immune Response and Cancer Progression. *Int J Mol Sci* **20**, doi:10.3390/ijms20122970 (2019).

16 Jiao, W. *et al.* Distinct downstream signaling and the roles of VEGF and PlGF in high glucose-mediated injuries of human retinal endothelial cells in culture. *Sci Rep* **9**, 15339, doi:10.1038/s41598-019-51603-0 (2019).

17 Lazzara, F. *et al.* Aflibercept regulates retinal inflammation elicited by high glucose via the PlGF/ERK pathway. *Biochem Pharmacol* **168**, 341-351, doi:10.1016/j.bcp.2019.07.021 (2019).

18 Huang, H. *et al.* Placental growth factor negatively regulates retinal endothelial cell barrier function through suppression of glucose-6-phosphate dehydrogenase and antioxidant defense systems. *FASEB J* **33**, 13695-13709, doi:10.1096/fj.201901353R (2019).

19 Valenzuela, D. M. *et al.* Angiopoietins 3 and 4: diverging gene counterparts in mice and humans. *Proc Natl Acad Sci U S A* **96**, 1904-1909, doi:10.1073/pnas.96.5.1904 (1999).

20 Nguyen, Q. D. *et al.* The Tie2 signaling pathway in retinal vascular diseases: a novel therapeutic target in the eye. *Int J Retina Vitreous* **6**, 48, doi:10.1186/s40942-020-00250-z (2020).

21 Whitehead, M., Osborne, A., Widdowson, P. S., Yu-Wai-Man, P. & Martin, K. R. Angiopoietins in Diabetic Retinopathy: Current Understanding and Therapeutic Potential. *J Diabetes Res* **2019**, 5140521, doi:10.1155/2019/5140521 (2019).

22 Suri, C. *et al.* Requisite role of angiopoietin-1, a ligand for the TIE2 receptor, during embryonic angiogenesis. *Cell* **87**, 1171-1180, doi:10.1016/s0092-8674(00)81813-9 (1996).

23 Jeansson, M. *et al.* Angiopoietin-1 is essential in mouse vasculature during development and in response to injury. *J Clin Invest* **121**, 2278-2289, doi:10.1172/JCI46322 (2011).

24 Yuan, H. T., Khankin, E. V., Karumanchi, S. A. & Parikh, S. M. Angiopoietin 2 is a partial agonist/antagonist of Tie2 signaling in the endothelium. *Mol Cell Biol* **29**, 2011-2022, doi:10.1128/MCB.01472-08 (2009).

25 Teichert, M. *et al.* Pericyte-expressed Tie2 controls angiogenesis and vessel maturation. *Nat Commun* **8**, 16106, doi:10.1038/ncomms16106 (2017).

26 Patel, J. I., Hykin, P. G., Gregor, Z. J., Boulton, M. & Cree, I. A. Angiopoietin concentrations in diabetic retinopathy. *Br J Ophthalmol* **89**, 480-483, doi:10.1136/bjo.2004.049940 (2005).

27 Lip, P. L. *et al.* Plasma vascular endothelial growth factor, angiopoietin-2, and soluble angiopoietin receptor tie-2 in diabetic retinopathy: effects of laser photocoagulation and angiotensin receptor blockade. *Br J Ophthalmol* **88**, 1543-1546, doi:10.1136/bjo.2004.048587 (2004).

28 Hammes, H. P. *et al.* Angiopoietin-2 causes pericyte dropout in the normal retina: evidence for involvement in diabetic retinopathy. *Diabetes* **53**, 1104-1110, doi:10.2337/diabetes.53.4.1104 (2004).

29 Rangasamy, S., Srinivasan, R., Maestas, J., McGuire, P. G. & Das, A. A potential role for angiopoietin 2 in the regulation of the blood-retinal barrier in diabetic retinopathy. *Invest Ophthalmol Vis Sci* **52**, 3784-3791, doi:10.1167/iovs.10-6386 (2011).

30 Khalaf, N. *et al.* Role of Angiopoietins and Tie-2 in Diabetic Retinopathy. *Electron Physician* **9**, 5031-5035, doi:10.19082/5031 (2017).

31 Wimmer, R. A. *et al.* Human blood vessel organoids as a model of diabetic vasculopathy. *Nature* **565**, 505-510, doi:10.1038/s41586-018-0858-8 (2019).

32 Lennikov, A. *et al.* Synergistic interactions of PlGF and VEGF contribute to blood-retinal barrier breakdown through canonical NFkappaB activation. *Exp Cell Res* **397**, 112347, doi:10.1016/j.yexcr.2020.112347 (2020).

33 Huang, H., Parlier, R., Shen, J. K., Lutty, G. A. & Vinores, S. A. VEGF receptor blockade markedly reduces retinal microglia/macrophage infiltration into laser-induced CNV. *PLoS One* **8**, e71808, doi:10.1371/journal.pone.0071808 (2013).

34 Huang, H., Shen, J. & Vinores, S. A. Blockade of VEGFR1 and 2 suppresses pathological angiogenesis and vascular leakage in the eye. *PLoS One* **6**, e21411, doi:10.1371/journal.pone.0021411 (2011).

35 Wimmer, R. A., Leopoldi, A., Aichinger, M., Kerjaschki, D. & Penninger, J. M. Generation of blood vessel organoids from human pluripotent stem cells. *Nat Protoc* **14**, 3082-3100, doi:10.1038/s41596-019-0213-z (2019).

36 Giaever, I. & Keese, C. R. Micromotion of mammalian cells measured electrically. *Proceedings of the National Academy of Sciences of the United States of America* **88**, 7896-7900 (1991).

37 Huang, H. *et al.* Reduced retinal neovascularization, vascular permeability, and apoptosis in ischemic retinopathy in the absence of prolyl hydroxylase-1 due to the prevention of hyperoxia-induced vascular obliteration. *Investigative ophthalmology & visual science* **52**, 7565-7573, doi:10.1167/iovs.11-8002 (2011).

38 Saddala, M. S. *et al.* Discovery of novel L-type voltage-gated calcium channel blockers and application for the prevention of inflammation and angiogenesis. *J Neuroinflammation* **17**, 132, doi:10.1186/s12974-020-01801-9 (2020).

39 Saddala, M. S., Lennikov, A., Mukwaya, A. & Huang, H. Transcriptome-Wide Analysis of CXCR5 Deficient Retinal Pigment Epithelial (RPE) Cells Reveals Molecular Signatures of RPE Homeostasis. *Biomedicines* **8**, doi:10.3390/biomedicines8060147 (2020).

40 Verbeke, G. & Molenberghs, G. *Linear Mixed Models for Longitudinal Data*. (New York: Springer-Verlag, Inc, 2000).

41 Sweeney, M. & Foldes, G. It Takes Two: Endothelial-Perivascular Cell Cross-Talk in Vascular Development and Disease. *Front Cardiovasc Med* **5**, 154, doi:10.3389/fcvm.2018.00154 (2018).

42 Huang, H. Pericyte-Endothelial Interactions in the Retinal Microvasculature. *Int J Mol Sci* **21**, doi:10.3390/ijms21197413 (2020).

43 Piera-Velazquez, S. & Jimenez, S. A. Endothelial to Mesenchymal Transition: Role in Physiology and in the Pathogenesis of Human Diseases. *Physiol Rev* **99**, 1281-1324, doi:10.1152/physrev.00021.2018 (2019).

44 Bischoff, J. Endothelial-to-Mesenchymal Transition. *Circ Res* **124**, 1163-1165, doi:10.1161/CIRCRESAHA.119.314813 (2019).

45 Wheelock, M. J., Shintani, Y., Maeda, M., Fukumoto, Y. & Johnson, K. R. Cadherin switching. *J Cell Sci* **121**, 727-735, doi:10.1242/jcs.000455 (2008).

46 Lennikov, A., Mukwaya, A., Saddala, M. S. & Huang, H. Deficiency of C-X-C chemokine receptor type 5 (CXCR5) gene causes dysfunction of retinal pigment epithelium cells. *Lab Invest* **101**, 228-244, doi:10.1038/s41374-020-00491-4 (2021).

47 Caporali, A. *et al.* Contribution of pericyte paracrine regulation of the endothelium to angiogenesis. *Pharmacol Ther* **171**, 56-64, doi:10.1016/j.pharmthera.2016.10.001 (2017).

48 Gavard, J. & Gutkind, J. S. VEGF controls endothelial-cell permeability by promoting the beta-arrestin-dependent endocytosis of VE-cadherin. *Nat Cell Biol* **8**, 1223-1234, doi:10.1038/ncb1486 (2006).

49 Gavard, J., Patel, V. & Gutkind, J. S. Angiopoietin-1 prevents VEGF-induced endothelial permeability by sequestering Src through mDia. *Dev Cell* **14**, 25-36, doi:10.1016/j.devcel.2007.10.019 (2008).

50 Cai, J., Kehoe, O., Smith, G. M., Hykin, P. & Boulton, M. E. The angiopoietin/Tie-2 system regulates pericyte survival and recruitment in diabetic retinopathy. *Invest Ophthalmol Vis Sci* **49**, 2163-2171, doi:10.1167/iovs.07-1206 (2008).

51 Milam, K. E. & Parikh, S. M. The angiopoietin-Tie2 signaling axis in the vascular leakage of systemic inflammation. *Tissue Barriers* **3**, e957508, doi:10.4161/21688362.2014.957508 (2015).

52 Duran, E. K. *et al.* Plasma Placental Growth Factor Concentrations Are Elevated Well in Advance of Type 2 Diabetes Mellitus Onset: Prospective Data From the WHS. *J Am Heart Assoc* **8**, e012790, doi:10.1161/JAHA.119.012790 (2019).

53 Al Kahtani, E. *et al.* Vitreous levels of placental growth factor correlate with activity of proliferative diabetic retinopathy and are not influenced by bevacizumab treatment. *Eye (Lond)* **31**, 529-536, doi:10.1038/eye.2016.246 (2017).

54 Mesquita;, J. *et al.* Comparison of serum and vitreous PIGF in diabetic retinopathy patients and non-diabetic patients. *IOVS* **56**, ARVO abstract 5179 (2015).

55 Suzuma, K. *et al.* Vascular endothelial growth factor induces expression of connective tissue growth factor via KDR, Flt1, and phosphatidylinositol 3-kinase-akt-dependent pathways in retinal vascular cells. *J Biol Chem* **275**, 40725-40731, doi:10.1074/jbc.M006509200 (2000).

56 Wu, J. H. *et al.* Inhibition of Sema4D/PlexinB1 signaling alleviates vascular dysfunction in diabetic retinopathy. *EMBO Mol Med* **12**, e10154, doi:10.15252/emmm.201810154 (2020).

57 Liu, D. *et al.* Erythropoietin maintains VE-cadherin expression and barrier function in experimental diabetic retinopathy via inhibiting VEGF/VEGFR2/Src signaling pathway. *Life Sci* **259**, 118273, doi:10.1016/j.lfs.2020.118273 (2020).

Figures

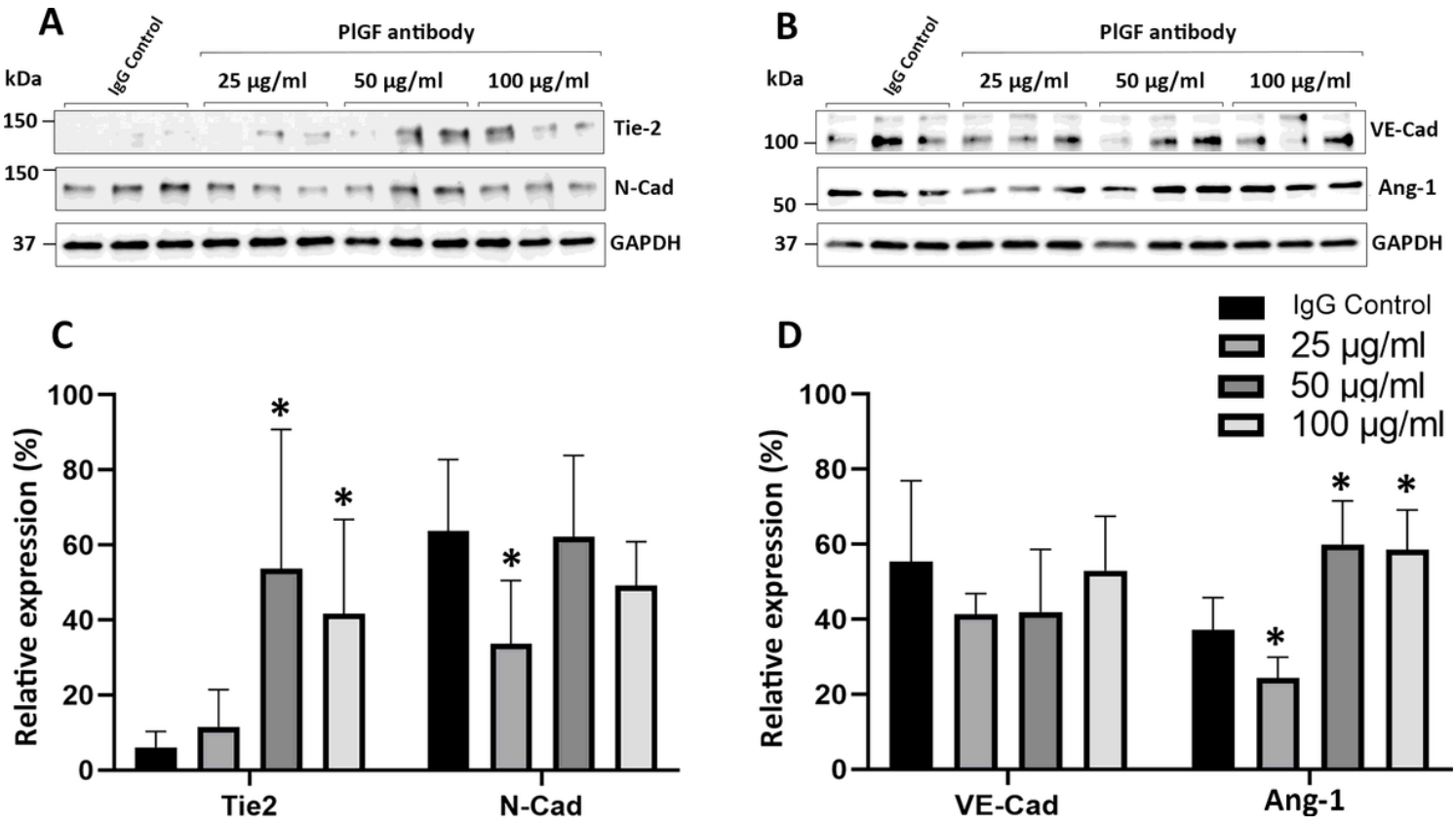

Figure 1

PlGF blockade regulates Ang-1 and Tie-2 protein expressions in HRP-HREC coculture in an antibody dose-dependent manner. Primary human retinal endothelial cells (HREC) and pericytes (HRP) are cocultured at a 2:1 ratio. The confluent HRP-HREC cocultures were treated with three PlGF antibody concentrations (25, 50, and 100 µg/ml) for two days. IgG was used as a treatment control. (A & B) Western blotting results of Tie-2, N-Cadherin (N-Cad), VE-Cadherin (VE-Cad), and Angiopoietin-1 (Ang-1). GAPDH acted as a loading control. Note that the HREC-HRP cocultures were used for all western blotting analyses. (C & D) Densitometry quantification results of the western blots. * indicates $P < 0.05$ compared with control. It should be noted: although the Tie-2 and Ang-1 WB results had variations (SD) among the three samples of 100 µg/ml PlGF antibody, the pixel intensities detected by Image J software were greater than any of the three controls, and thereby the ANOVA analysis leads to a statistically significant result ($p = 0.0408$ for Ang-1; $p = 0.0113$ for Ang-1).

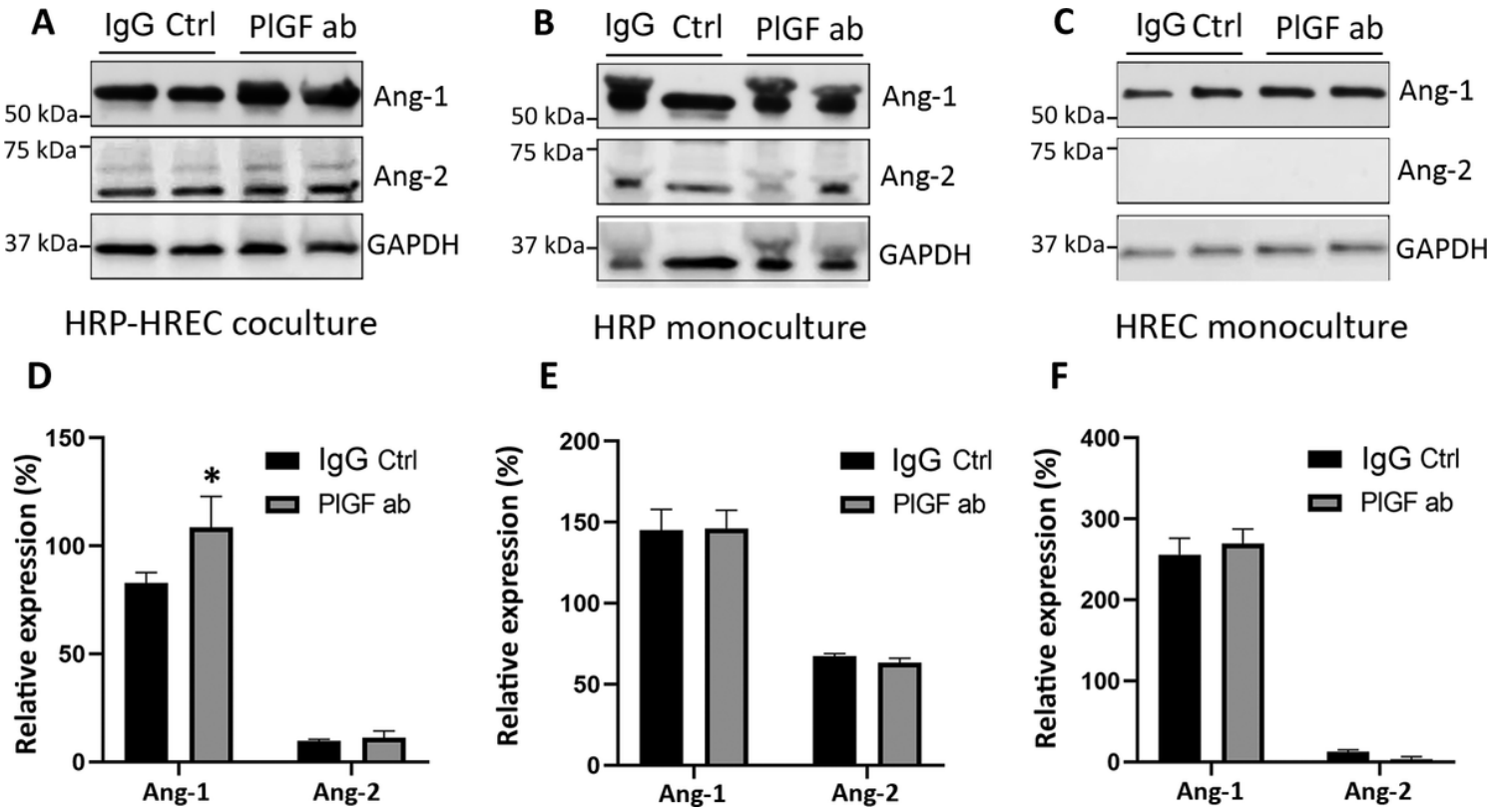

Figure 2

Ang-1 upregulation caused by PlGF blockade requires HRP-HREC interactions. Primary human retinal endothelial cells (HREC) and pericytes (HRP) are cultured alone or cocultured as described in methods. IgG and PlGF antibody (50 μg/ml) treated the confluent coculture and monoculture for two days. Western blots (WB) and densitometry analysis were performed to determine the protein expression. WB results of HRP-HREC coculture (A), HRP monoculture (B), and HREC monoculture (C). Densitometry quantification results of HRP-HREC coculture (D), HRP monoculture (E), and HREC monoculture (F). The results were expressed a relative expression to the housekeeping protein (GAPDH).* indicates $P < 0.05$ compared with IgG control.

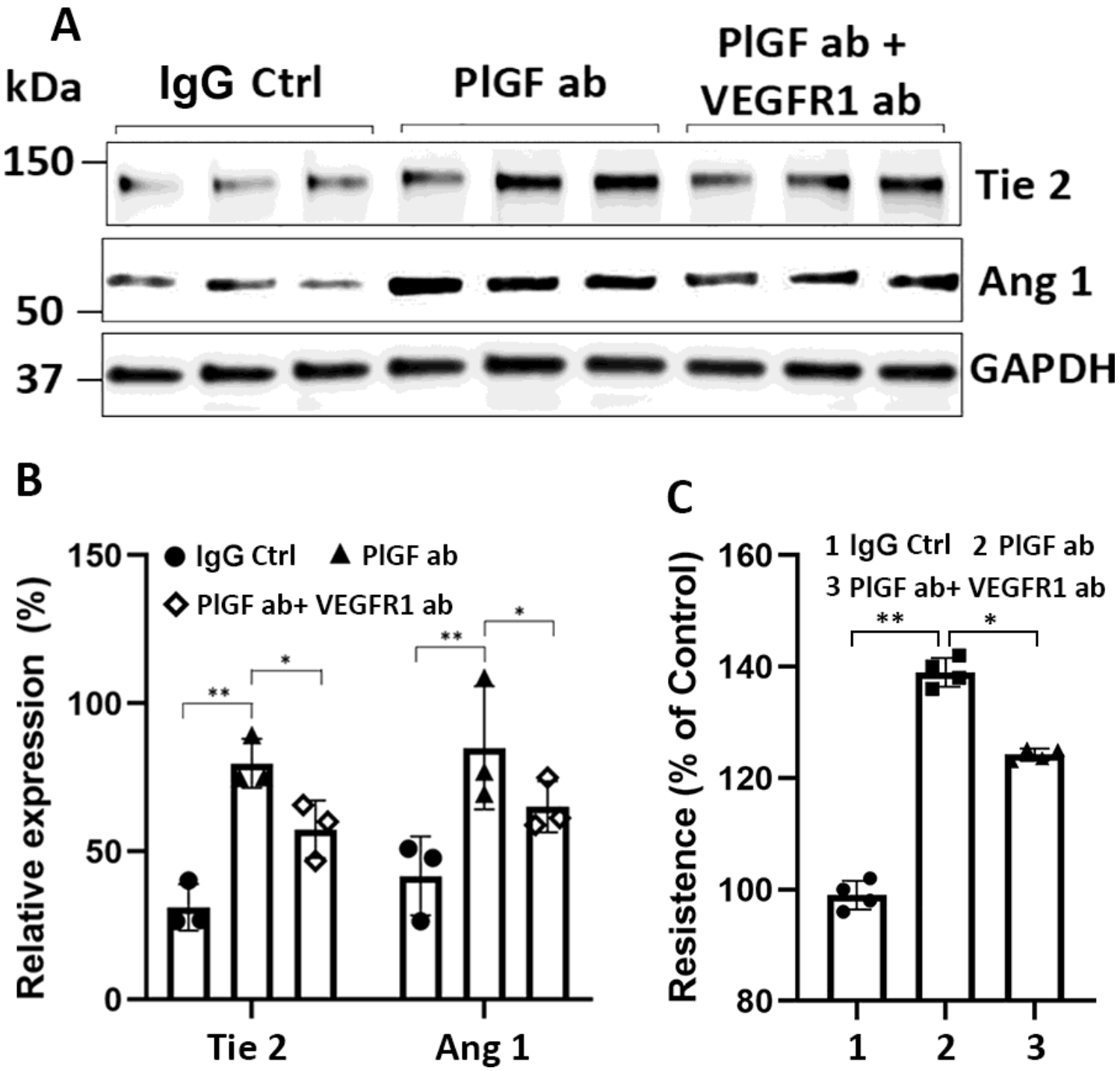

Figure 3

VEGFR1 inhibition diminishes PlGF's effect on Ang-1 and Tie-2 expression in HREC-HRP coculture. HREC and HRP were cocultured and treated with three groups: IgG control, PlGF antibody (ab) (50 μg/ml), and PlGF ab (50 μg/ml) + VEGFR1 ab (50 μg/ml). The western blots (A) and densitometry quantification results (B). GAPDH was used as a protein loading control. (C) Resistance results were measured with the ECIS system. The results were expressed as a percentage relative to control (mean ± SD, n = 3 for WB, n = 4 for resistance). * $P < 0.05$. ** $P < 0.01$.

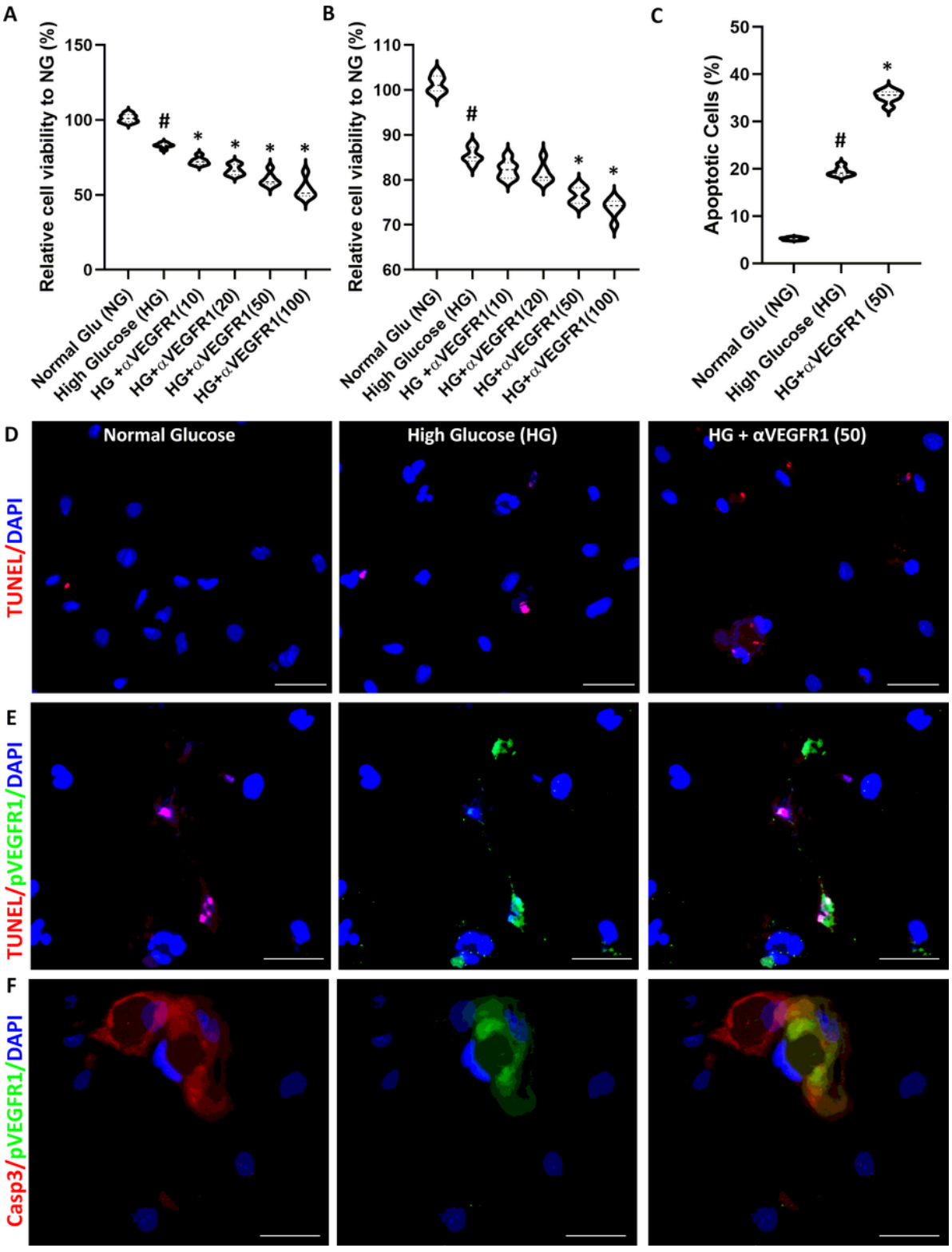

Figure 4

VEGFR1 inhibition reduces pericyte viability in high-glucose conditions. The pericytes were cultured with normal glucose (NG), high glucose (HG), and HG + varying VEGFR1 antibody concentrations (10, 20, 50, and 100 µg/ml). The cell lysates were used for cell viability assay with MTT (A) and the supernatant for LDH assay (B). The results were expressed as relative cell viability to NG (mean ±SD, n=6). (C and D) The TUNEL (+) apoptotic cells were counted for NG, HG, and HG + 50 µg/ml VEGFR1 antibody. # P < 0.05

(compared to normal glucose). * P < 0.05 (compared to high glucose). (E, F) Double immunofluorescent labeling was performed for: pVEGFR1 and TUNEL (E), activated Caspase 3 (a-Casp3), and pVEGFR1 (F). Scale bar: 50 μm. Note that pVEGFR1 staining signals were co-localized with the TUNEL(+) and a-Casp3 (+) apoptotic cells.

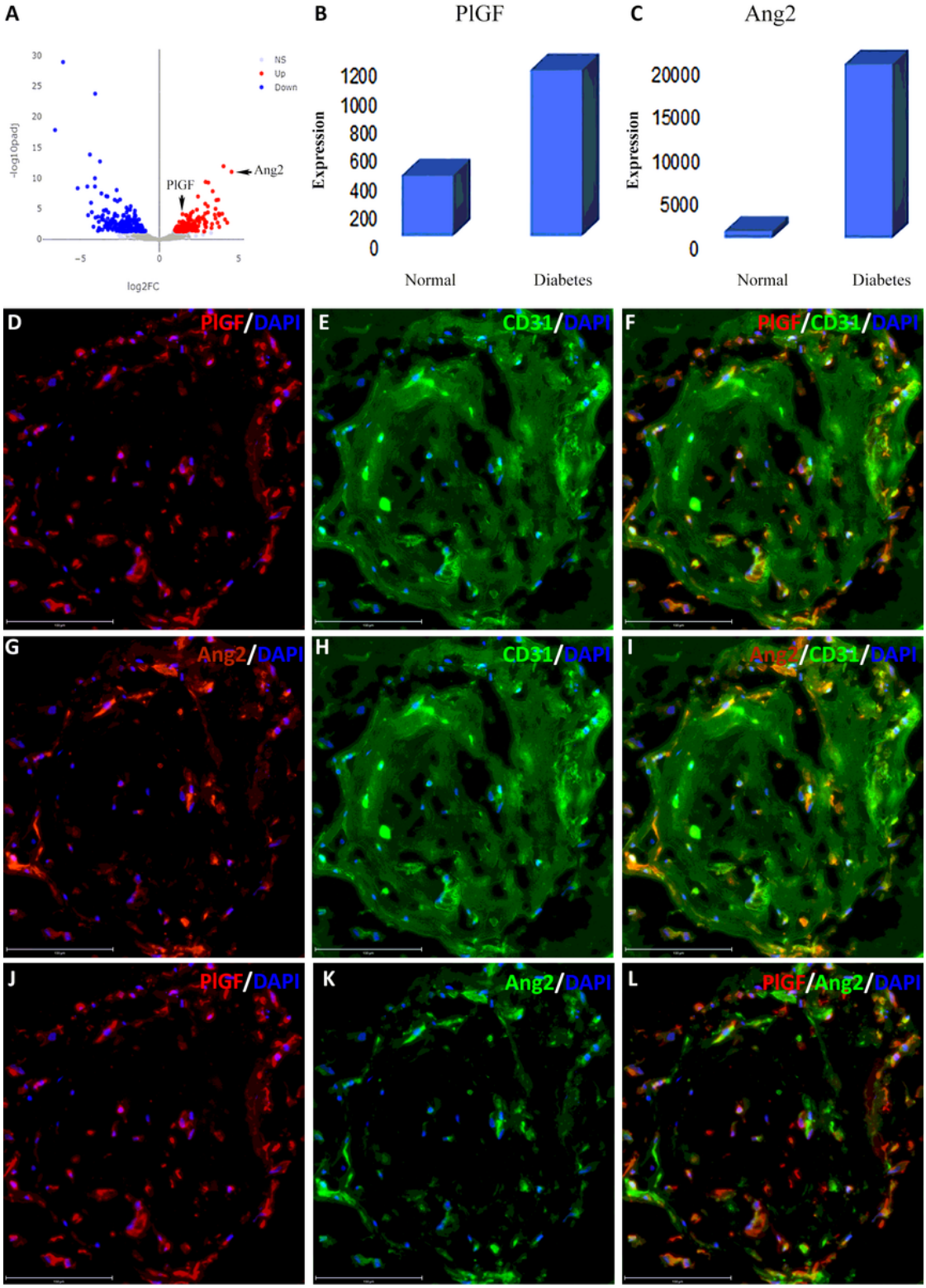

Figure 5

PlGF is expressed in perivascular (pericyte) cells and upregulated by diabetes-mimicking conditions in the human iPSC-derived vascular organoids. (A-C) Bioinformatic analysis of RNA sequencing data revealed PlGF and Ang2 were upregulated by diabetes-mimicking conditions. Volcano plot (A) showed the differentially expressed genes between normal and diabetic conditions, in which arrows indicated PlGF and Ang2. Their expression levels were shown in PlGF (B) and Ang2 (C). (D-L) Double labeling revealed PlGF and Ang2 had a perivascular (pericyte) localization in the human iPSC-derived vascular organoids. Scale bar: 150 μm.

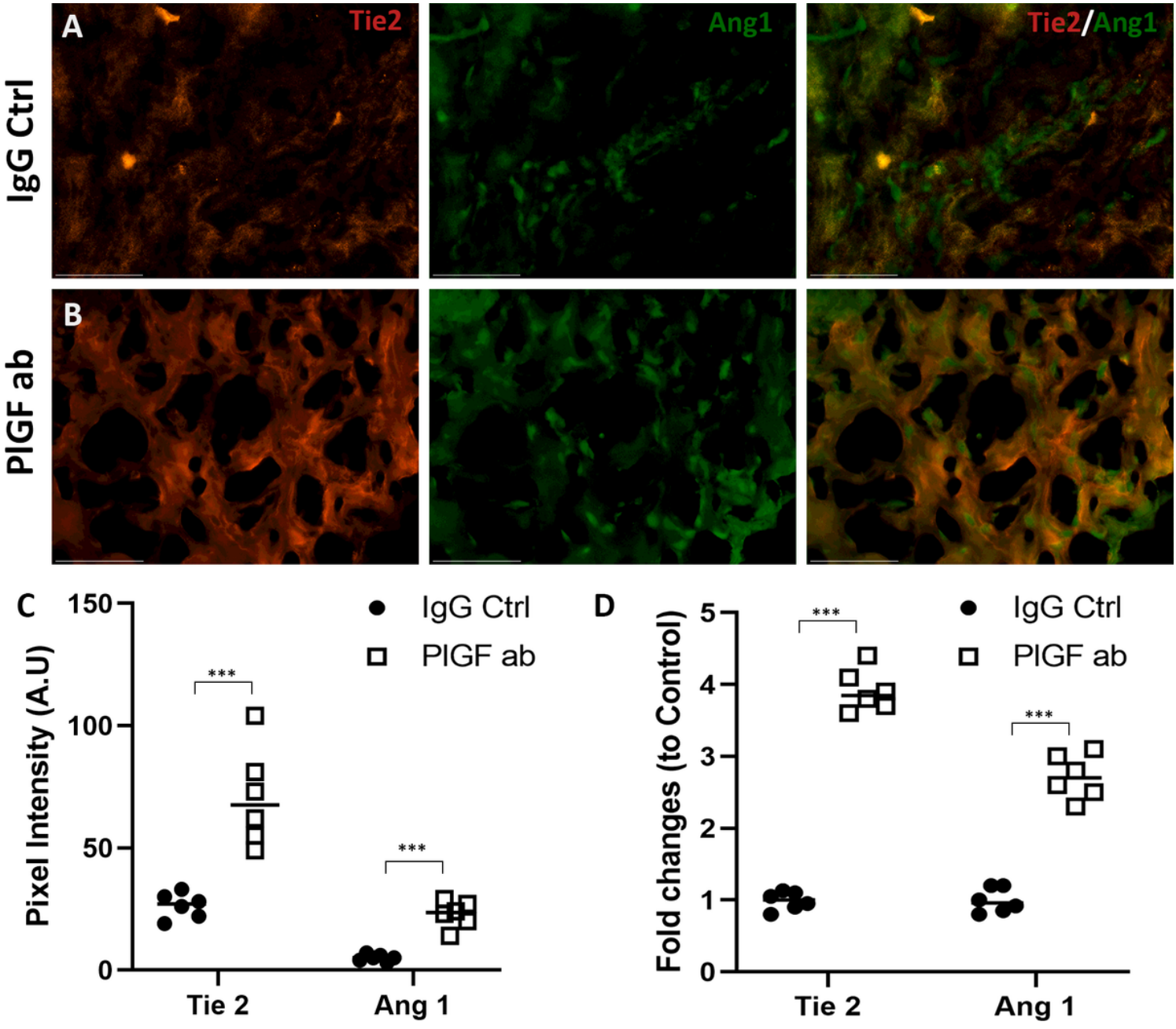

Figure 6

PlGF blockade upregulates Ang-1 and Tie-2 in human iPSC-derived vascular organoids. Vascular organoids were generated from human iPSC as described in methods. 100 μg/ml PlGF antibody was supplemented into the culture medium and incubated for 4 days. IgG was used as a control. 10-micron

cryopreserved sections were made for immunofluorescent staining with anti-Ang-1 and anti-Tie-2 antibodies. The secondary antibodies with Alex Fluor 647 (infrared) and 488 (green) were used for visualization and microphotography with EVOS M7000 fluorescent microscope (A, B). Scale bar: 75 μm. (C) Quantification results of the fluorescent images measured with ImageJ software (n = 6). *** P < 0.0001. The fluorescent images from each channel were made with the same exposure time for both control and antibody treatment conditions to minimize the variations caused by the fluorescent imaging process. The expression levels were measured based on the mean pixel intensity per image (6 images in total). The two additional example images used for quantification were shown in Suppl. Fig. 4. Note that Ang-1 had a peri-vascular (pericyte) expression pattern similar to PlGF and Ang2. (D) qRT-PCR results of Tie-2 and Ang-1 mRNA transcripts. The values represent the change folds relative to control (n = 6). *** P < 0.0001.

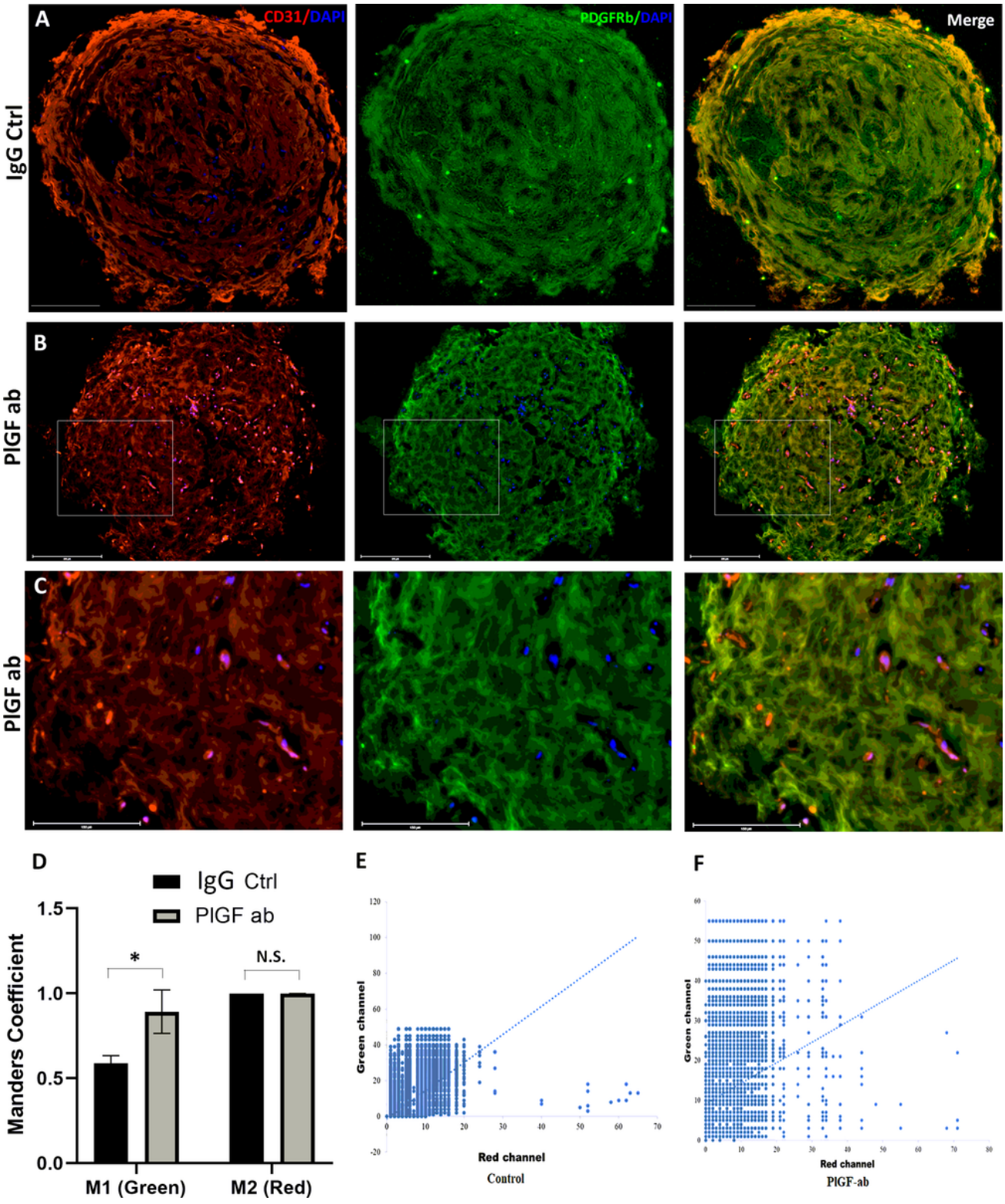

Figure 7

PlGF blockade promotes the pericytes coverage and association with ECs in vascular organoids. Vascular organoids (VO) were derived from human iPSC-derived. The VO micrographs double-stained with CD31 (red channel) and PDGFRb (green channel) were processed for colocalization analysis with Image J software and the JACop plugin. (A and B) The micrographs were from the control group (A) and PlGF antibody treatment (B). Scale bar: 275 μm. (C) The box areas in Panel B showed the colocalization of

CD31 (red) and PDGFRb (green). Scale bar: 150 μm. (D) The Manders' overlay coefficients indicate the degree of colocation: M1 stands for the green (PDGFRb+ pericytes), and M2 for the red (CD31+ EC). The values were expressed as mean percentage ± SD (n = 3). * indicates p <0.05. N.S: Non-Significance. (E and F) Cytofluorogram showed the Pearson correlation coefficients between the green and red channels (E: IgG control; F: PlGF ab).

Supplementary Files

This is a list of supplementary files associated with this preprint. Click to download.

- SupplFig.1.tif
- Suppl.Fig.2.tif
- Suppl.Fig.3.tif
- Suppl.Fig.4.tif
- Suppl.Fig.5.tif
- Suppl.Fig.6.tif